chemosensors

MDPI

Communication

A Ratiometric Selective Fluorescent Probe Derived from Pyrene for Cu^{2+} Detection

Chunwei Yu [1,2,3,†], Mei Yang [4,†], Shuhua Cui [5], Yuxiang Ji [1] and Jun Zhang [1,2,3,*]

1 School of Tropical Medicine, Hainan Medical University, Haikou 571199, China; hy0211045@hainmc.edu.cn (C.Y.); hy0211012@hainmc.edu.cn (Y.J.)
2 Key Laboratory of Tropical Translational Medicine of Ministry of Education, Hainan Medical University, Haikou 571199, China
3 NHC Key Laboratory of Control of Tropical Diseases, School of Tropical Medicine, Hainan Medical University, Haikou 571199, China
4 School of Public Health and One Health, Hainan Medical University, Haikou 571101, China; yang24364@hainmc.edu.cn
5 School of Chemical Engineering and Environment, Weifang University of Science and Technology, Shouguang 262700, China; cuishuhua@wfust.edu.cn
* Correspondence: hy0211049@hainmc.edu.cn
† These authors contributed equally to this work.

Abstract: A novel ratiometric Cu^{2+}-selective probe was rationally constructed based on pyrene derivative. Compared to other tested metal ions, the probe presented the selective recognition for Cu^{2+} which could be detected by a significant turn-on fluorescent response at 393 nm and 415 nm. Under the optimized conditions, a detection limit of 0.16 μM Cu^{2+} in aqueous media was found. Besides this, a 1:1 metal–ligand complex was confirmed by MS spectra and Job's plot experiment, and the binding mode was also studied by ^{1}H NMR experiment. Meanwhile, the fluorescence imaging in living cells was performed to detect Cu^{2+} with satisfactory results.

Keywords: Cu^{2+}; probe; pyrene; fluorescence imaging

Citation: Yu, C.; Yang, M.; Cui, S.; Ji, Y.; Zhang, J. A Ratiometric Selective Fluorescent Probe Derived from Pyrene for Cu^{2+} Detection. *Chemosensors* **2022**, *10*, 207. https://doi.org/10.3390/chemosensors10060207

Academic Editor: Camelia Bala

Received: 3 May 2022
Accepted: 27 May 2022
Published: 31 May 2022

1. Introduction

Because of wide use of heavy metal ions, analysis and detection of them has been an important means of disease prevention and control in public health and environmental safety [1,2]. Cu^{2+}, as an important heavy metal ion, is confirmed to be harmful to human health in that excessive concentration of Cu^{2+} is probably involved in the forming of reactive oxygen species to bring out neurodegenerative disorders, such as Wilson's diseases [3]. To prevent Cu^{2+}-related pollution and health problems, design of effective tools capable of detection of trace amounts of Cu^{2+} has inspired considerable interest. Due to these advantages, including rapid analysis, high sensitivity, real-time in situ monitoring, and high spatial resolution, fluorescence probe method is expected to be an ideal choice for sensing and bioimaging of analytes in a variety of samples [4–6]. To date, researchers have developed many Cu^{2+} fluorescent probes [7–9]. One of the most important approaches is that a specific group is grafted to a fluorophore by organic methods [10–12]. Zhao's group developed a Cu^{2+} fluorescent probe by incorporating benzoyl hydrazone group as a receptor into the fluorophore hemicyanine, which could rapidly recognize Cu^{2+} and was also used for cell image [13]. Li et al. synthesized a Cu^{2+} fluorescent probe by combining a specific recognition unit phenol derivative with a cyanine dye [14]. However, because Cu^{2+} is a fluorescence quencher due to its paramagnetic through energy or electron transfer processes, these probes showed an "on-off" fluorescence response [15–17]. Based on sensitivity and selectivity considerations for practical applications, fluorescence quenching probes upon Cu^{2+} combination are not as popular as fluorescence enhancement probes under Cu^{2+} binding. In contrast, "turn-on" fluorescent probes by Cu^{2+}-triggered have

attracted special interest. A number of these fluorescent probes have been synthesized and characterized [18–20]. For example, You's group reported a highly fluorescent probe derived from a quinoline moiety for Cu^{2+} in DMSO-Tris buffer and living cells [21]. In addition, some probes based on rhodamine derivatives could recognize Cu^{2+} with the aid of structural changes between spirolactam and ring-opened amide to gives rise to a stronger fluorescence emission and color change [22]. However, these limitations, including organic cosolvent dependence, poor photostability, poor cellular compatibility and pH dependence [23,24], to some extent, lowered the sensitivity and also restricted the practical applications because the recognition groups had drawbacks in selectivity and sensitivity. Therefore, development of highly selective and sensitive fluorescent probes for Cu^{2+} sensing with "off-on" response has been still of great challenge.

With this in mind, in this study, probe P was reasonably constructed by connecting an important fluorophore pyrene with 2-aminobenzhydrazide via –C=N– bond (Scheme 1). The responses of P toward Cu^{2+} were explored in detail by UV and fluorescence analysis. P was also demonstrated that it could react with Cu^{2+} and effectively turn on fluorescence in living cells. The design concept was explained as follows: (1) Pyrene was used as the fluorophore in view of its excellent photophysical properties and easy modification on the molecular structure [25,26]. In particular, its fine structures of excited state were the ideal signal units for construction of ratio-type fluorescent probes, which measure the ratio of fluorescence intensity at two different wavelengths as a signal parameter. This mode is not affected by the intensity of light source and instrument; (2) Acylhydrazone Schiff base was one of most selective π-conjugated reagents for Cu^{2+}. In addition, this type of compound was characterized by ketone–enol tautomerism, and O atom of the carbonyl group (–C=O), N atom of the amino group ($–NH_2$), and the imine group (–N=CH) could participate in coordination with Cu^{2+} and consequently produced stable coordination complexes according to HSAB principle [27]; (3) C=N isomerization and photoinduced electron-transfer (PET) phenomenon were introduced as common signaling mechanisms to play roles in photophysical processes upon binding of P with Cu^{2+}, which was based on the following considerations. Firstly, the main advantage was that it was easy to prepare and design "off-on" probes based on the two mechanisms; furthermore, the affinity of the chelating group C=N for heavy metal ions was stronger than that for alkali metals and alkaline earth metals [28,29].

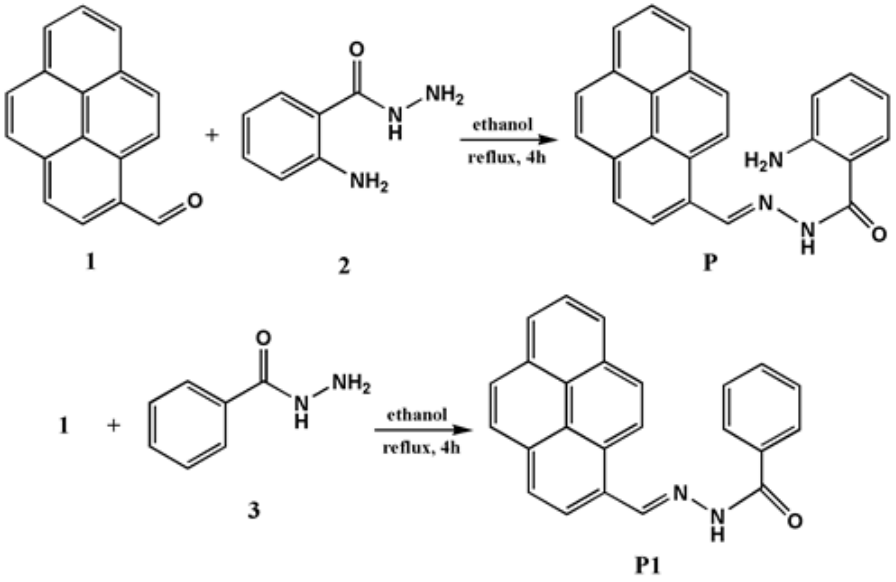

Scheme 1. Design and synthesis of compounds.

2. Materials and Methods

2.1. Materials and Instruments

All reagents used in our study were all analytically pure and used directly.

Fluorescence experiments were carried out by a Hitachi 4600 spectrofluometer (Japan). Absorption spectra were measured by a Hitachi U-2910 spectrophotometer (Japan). Confocal microscopy imaging was determined in an Olympus FluoView Fv3000 laser scanning microscope (Japan). Electrospray ionization (ESI) analyses were performed on a Thermo TSQ Quantum Mass Spectrometer (America), method parameters: Sheath Gas Flow Rate (arb): 30; Aux Gas Flow Rate (arb): 10; Capillary Temp. (°C): 275; Capillary Voltage (V): −45.00 (ES−)/10.00 (ES+); SpraVoltage (kV): 5.00. ^{1}H NMR and ^{13}C NMR spectra were performed by a Bruker AV 400 instrument with tetramethylsilane (TMS) as an internal standard and DMSO-d_6 as a deuterium generation reagent (Switzerland).

2.2. Synthesis of P and P1

0.23 g (1 mmol) compound 1 and 0.158 g (1 mmol) compound 2 were stirred in ethanol (40 mL) and refluxed for 4 h, and then cooled slowly to 25 °C, followed by filtering precipitate so produced. The obtained yellow solid P was dried and used directly. Yields: 83.4%. MS (ESI+) m/z: 364.1 $[M + H]^+$, 386.6 $[M + Na]^+$. ^{1}H NMR (δ ppm, d_6-DMSO): 11.80 (s, 1H), 9.46 (s, 1H), 8.81 (d, 1H, J = 7.25), 8.58 (d, 1H, J = 7.72), 8.37 (d, 1H, J = 7.88), 8.27 (d, 1H, J = 8.88), 8.23 (d, 1H, J = 8.92), 8.13 (t, 1H, J = 7.62), 7.72 (d, 1H, J = 7.72), 7.28 (t, 1H, J = 7.60), 6.74 (d, 1H, J = 8.24), 6.67 (t, 1H, J = 7.42), 6.47 (b, 2H). 13C NMR (δ ppm, d_6-DMSO): 151.11, 146.48, 133.27, 132.67, 131.78, 131.08, 129.57, 129.42, 129.19, 128.31, 128.12, 127.47, 126.94, 126.61, 126.13, 125.88, 125.09, 124.72, 123.41, 117.41, 115.59 (Figures S1–S3).

Compound P1 was synthesized similar to P. Yields: 87.2%. MS (ESI+) m/z: 349.3 $[M + H]^+$, 371.2 $[M + Na]^+$ (Figure S4).

2.3. Optical Experimental Method

Stock solutions of metal ions and compound P/P1 were prepared by dissolving appropriate amount in deionized water and DMSO, respectively. Slit widths of excitation and emission were 5 nm and 5 nm, respectively. Excitation wavelength was 350 nm.

2.4. Cell Culture

Hela cells were washed 3 times by PBS (phosphate-buffered saline), and incubated with 1 μM of Cu^{2+} (in PBS) for 30 min at 37 °C, followed by washing another 3 times with PBS. Then, 10 μM of probe P (in DMSO) was added. After treatment for 30 min in the same growth media, it was washed 3 times with PBS again.

Other cell culture experiments were completed according to this method mentioned above.

The cytotoxicity experiment of P in Hela cells was measured using MTT assay. Cells were seeded into 96-well cell culture plate at a rate of 4000/well in 5% CO_2 at 37 °C for 24 h, followed by adding probe P (0, 0.1, 1, 10 μM), and then allowed to incubate for 24 h, respectively. Subsequently, each well was injected with 20 μL MTT (5 mg/mL) and cultured for another 4 h under the same conditions. After that, cells were lysed in the solution composed of 10% SDS, 0.012 M HCl, and 5% isopropanol. A_{570nm} of each well was obtained on a microplate reader to calculate the amount of formazan.

3. Results

3.1. Effects of pH

Effect of pH was firstly investigated to evaluate the actual sensing for Cu^{2+}. The results were displayed in Figure 1, when Cu^{2+} was not added to the P solution, the fluorescence intensity of P itself remained fairly static in the range of pH 4–10. However, after mixing P with Cu^{2+}, the emission intensity gradually increased in the range of pH 4–7, which reached a maximum at pH 6.3. While pH > 7, the fluorescence intensity began to decrease, which tended to the formation of $Cu(OH)_2$ precipitation. Thereby, the pH-control measurements

revealed that P was stable in a wide range of pH, which also showed P had the best sensing response to Cu^{2+} at pH 6.3. All measurements were carried out in alcohol–aqueous media (v/v, 8:2, pH 6.3, 0.02 M HEPES).

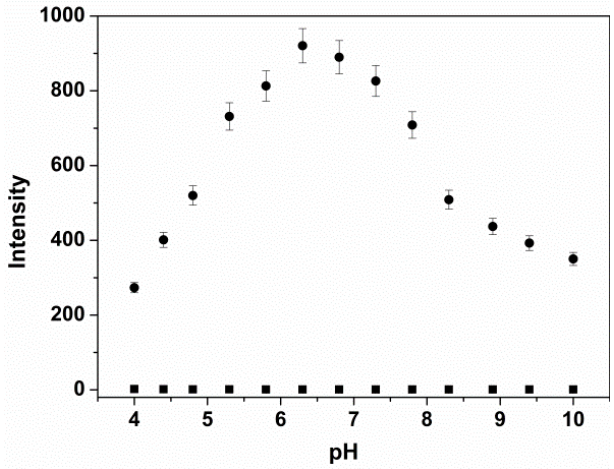

Figure 1. pH-dependent fluorescence response of P (10 μM) and P (10 μM) toward Cu^{2+} (100 μM) under different HEPES buffers.

3.2. UV-Vis Response of P

Absorption spectra of P to various common metal ions were illustrated in Figure 2. P exhibited three absorption bands with peaks at 400 nm, 380 nm and 280 nm, we attributed it to the electron transition of pyrene in the energy bond of π-π* and n-π*. Upon the addition of general metal ions (100 μM), such as K^+, $Na^{+,}$ Ca^{2+}, Mg^{2+}, Zn^{2+}, Pb^{2+}, Cd^{2+}, Cr^{3+}, Co^{2+}, Ni^{2+}, Hg^{2+}, Cu^{2+} and Ag^+; only Cu^{2+} resulted in an appreciable spectral change with three new blue-shifted absorption peaks at 340 nm, 325 nm and 275 nm. In addition, absorbance enhancement at 275 nm was also obvious (Figure 2a). These results were enough to account for the binding between P and Cu^{2+}.

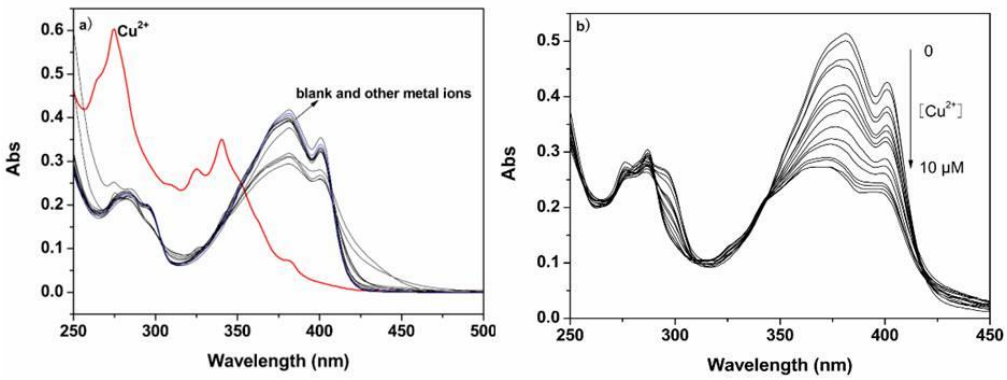

Figure 2. Absorption spectra. (**a**) absorption spectra of P (10 μM) toward metal ions (100 μM) in alcohol–aqueous media (v/v, 8:2, pH 6.3, 0.02 M HEPES); (**b**) absorption titration of P (10 μM) upon addition of increasing amounts of Cu^{2+} (0–10 μM) under the same conditions.

The absorption titration experiment showed a significant decrease of absorbance at 400 nm, 380 nm, and an absorbance increase at 275 nm was observed simultaneously with three isosbestic points at 290 nm, 310 nm and 340 nm, which displayed an obvious ratiometric absorbance change (Figure 2b). These results indicated that P possessed the characteristic of recognizing Cu^{2+} by ratio absorption spectrum, and it also be concluded that Cu^{2+} binding with P blocked conjugation of the double bonds and resulted in the appearance of some shorter absorption wavelengths.

3.3. Characterization of Fluorescent Response of P

The selective properties of P for respective metal ions were further evaluated by fluorescence spectroscopy. P itself showed a very weak fluorescence response with the excitation wavelength 350 nm as seen in Figure 3a, the reason was explained by the transfer of the lone pair electrons from –C=N– group to benzoyl hydrazine unit. In addition, it was likely due to non-radiative decay of the C=N bond in excited state. When comparing Cu^{2+} with other examined metal ions, a remarkable "turn-on" fluorescence response generated at 393 nm and 415 nm by the addition of Cu^{2+}, which was the typical monomer emission of pyrene. In this process, we surmised that the N and O atoms in Schiff base maybe participate in forming the complex P-Cu^{2+}, and the isomerization of C=N bond and PET process were restricted, so the enhanced fluorescence intensity at 393 nm and 415 nm were induced significantly. These results suggested that P could act as an ideal fluorescent probe for Cu^{2+} over other metal ions. Competitive experiments were also employed to prove the practical application of P as a Cu^{2+}-sensitive fluorescent probe. As shown in Figure S5, after Cu^{2+} was added to the mixture of P with different interfering substances, including Na^{+}, K^{+}, Mg^{2+}, Ca^{2+}, Pb^{2+}, Zn^{2+}, Cd^{2+}, Co^{2+}, Hg^{2+}, Cr^{3+}, Ag^{+} and Ni^{2+}, an obvious enhancement of the fluorescence intensity ratio (I_{393nm}/I_{415nm}) was caused. These results displayed that the fluorescence signal of P toward Cu^{2+} was not susceptible remarkably to the coexistent metal ions, which further confirmed that P was a promising probe to sense Cu^{2+}. Furthermore, to evaluate the role of amino group in P, the fluorescence signal of control compound P1 toward the above mentioned metal ions were also measured as seen in Figure 3b. No remarkable emission of P1 at 440 nm was observed, and an emission band at 393 nm and 415 nm was not shown upon addition of Cu^{2+} as found in P, which indicated the amino group played a crucial role in the formed chelating complex P-Cu^{2+}.

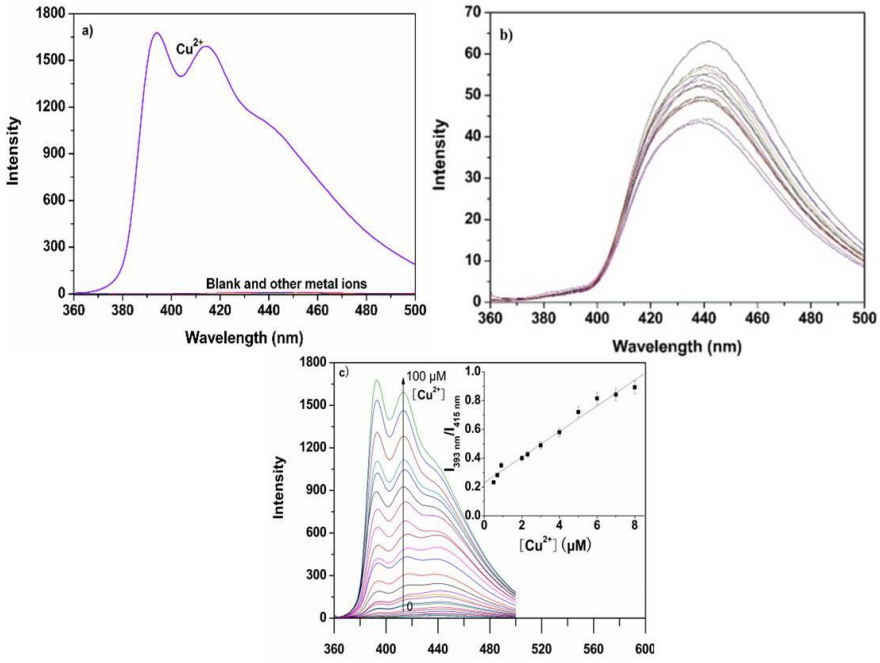

Figure 3. Fluorescence spectra. (**a**) fluorescence response of P (10 μM) to different metal ions (100 μM) in alcohol–aqueous media (*v*/*v*, 8:2, pH 6.3, 0.02 M HEPES); (**b**) fluorescence emission of P1 (10 μM) for above-mentioned metal ions (100 μM) in alcohol–aqueous media (*v*/*v*, 8:2, pH 6.3, 0.02 M HEPES); (**c**) fluorescence titration of P (10 μM) with various [Cu^{2+}], inset: the ratios of fluorescent emission intensity (I_{393nm}/I_{415nm}) of P (10 μM) as a function of [Cu^{2+}] within 0.5–8 μM.

The sensing ability of Cu^{2+} with P was also checked by the titration experiment with fluorescence spectroscopy. Along with the increasing concentration of Cu^{2+}, the fluorescence intensity at 393 nm and 415 nm enhanced gradually (Figure 3c), which indicated

a ratiometric fluorescence change. The linear fitting curve showed that a perfect linear relationship between the ratios of fluorescent emission intensity (I_{393nm}/I_{415nm}) and [Cu^{2+}] within 0.5–8 μM, and LOD (a detection limit) of 0.16 μM was obtained, respectively. It exhibited that probe P could be used for qualitative and quantitative sensing of Cu^{2+}, and the sensitivity reached 30 μM Cu^{2+} in drinking water in the standard of the WHO (World Health Organization) [30].

3.4. Reaction Mechanism Research

To explore the probable complexation between P and Cu^{2+}, we conducted Job's plot experiment as displayed in Figure 4 and Figure S6. A maximum emission intensity at 460 nm was found with the proportion of [P]/[Cu^{2+}] of 0.5. As expected, a 1:1 stoichiometry for the complex p-Cu^{2+} was indicated. It was also proved using the Benesi–Hildebrand method [31], the association constant (*Ka*) was approximately equal to 6.5 × 10^5 M^{-1} from fluorescence titration experiments (Figure S7), compared with reported Cu^{2+}-probe (2.18 × 10^4 M^{-1}) [32], and it indicated that a stable complex was formed between P with Cu^{2+}. Meanwhile, this 1:1 binding stoichiometric mode was also observed on MS spectra of P-Cu^{2+}, a peak at *m*/*z* 425.06 (ESI+) belonged to ([P + Cu^{2+}-H^+]$^+$) (Figure S8).

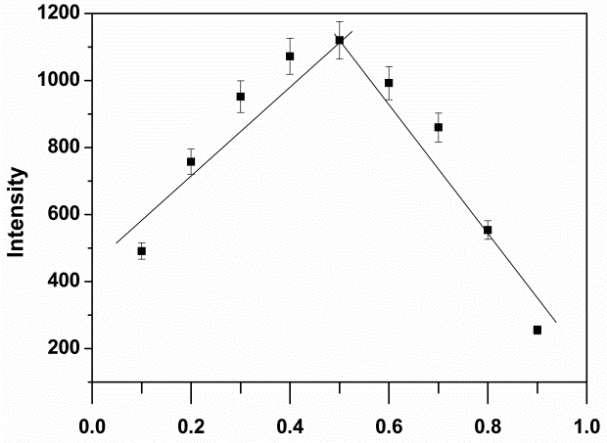

Figure 4. Stoichiometry for P and Cu^{2+} by Job's plot in alcohol–aqueous media (*v*/*v*, 8:2, pH 6.3, 0.02 M HEPES). The total concentration of ([P] + [Cu^{2+}]) was 10 μM.

To explore the binding mode of complex P-Cu^{2+} and also to fully strengthen the sensing mechanism of P with Cu^{2+}, ^{1}H NMR experiment was carried out as shown in Scheme 2. Free P showed the NMR signal of H_b, H_a, H_c at 11.803, 9.485, 6.486 ppm. Upon the addition of 1.0 equiv Cu^{2+}, the NMR signal of H_b (O=C–NH–) disappeared, while that of H_a (–CH=N), H_c (–NH_2) downshifted to 9.639 and 7.912, respectively. Meanwhile, the addition of Cu^{2+} promoted the NMR peaks in the range of 6.5–9.0 ppm, which assigned to protons of pyrene and phenyl to widen and combine together. It suggested that the structure of P became more rigid after coordination with Cu^{2+}.

Keeping these results in mind, a sensing mechanism for the complex P-Cu^{2+} was surmised as depicted as Scheme 2. According to the MS spectra of P-Cu^{2+} complex, 425.06 (ES+) belonged to [P + Cu^{2+}-H^+]$^+$, which proved the result that the formation of –OH enhanced the coordination ability of O, and a stable five-membered ring formed in the P-Cu^{2+} complex. Thus, –C=O, –NH_2 and –C=N groups participated in the coordination of P-Cu^{2+} complex. Moreover, the reaction of Cu^{2+} with P blocked the PET and C=N isomerization and greatly increased the emission intensity of pyrene moiety.

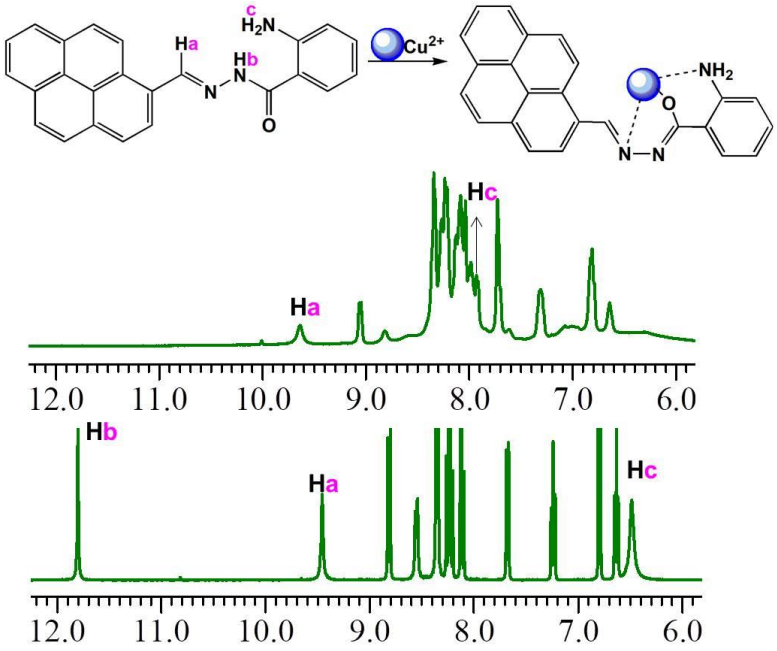

Scheme 2. Recognization mode between P and Cu^{2+}.

3.5. Cell Application

According to the excellent fluorescence properties of P, the application of P in living cells was explored. Firstly, cytotoxicity of P on Hela cells using a standard MTT assay was performed. As was shown in Figure S8, after the cells were incubated for 24 h with P concentrations within 0–10 μM, high celluar viability was still found to be about 95% (Figure S9), which demonstrated the low cytotoxicity and favorable biocompatibility of P to cultured Hela cells.

After that, the biological capability experiment of P to detect Cu^{2+} in Hela cells was conducted. When the Hela cells were supplemented with 10 μM of P at 37 °C for 30 min, a very faint fluorescence intensity was detected (Figure S5), suggesting that background signal in the cells was very feeble. In contrast, when cells treated with Cu^{2+} (1 μM) for 30 min, and then cultured upon addition of P (10 μM) for 30 min, a dramatic fluorescence change was triggered (Figure 5d), demonstrating that P had a good cell-membrane penetration, which also clearly displayed that the enhanced intracellular fluorescence change resulted from interaction of Cu^{2+} with P inside cells. We could deduce that P had low toxicity and good cytocompatibility in view of the morphology of cells. Hence, P may act as a prospective probe to image Cu^{2+} for bioanalysis.

In addition, fluorescence imaging of P (10 μM) with various [Cu^{2+}] (0, 2, 4, 6, 8 μM) in Hela cells was measured. It could be seen that the fluorescence intensity was enhanced regularly with increasing concentration of Cu^{2+} as shown in Figure 6a–e, which also determined based on the average fluorescence intensity by confocal laser scanning microscopy as displayed in Figure 6f. These data also established that P could respond to intracellular Cu^{2+} level changes in living cells.

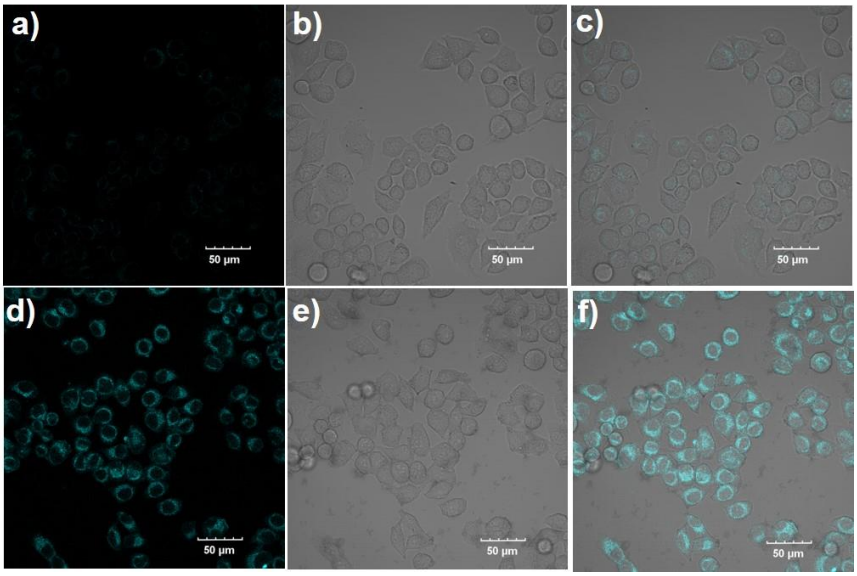

Figure 5. Hela cells fluorescence images. (**a**) cells cultured with 10 μM of P for 30 min in the growth medium; (**b**) image of bright field cells in panel (**a**); (**c**) images of overlay in panels (**a**,**b**); (**d**) after supplementing with 1 μM of Cu^{2+} for 30 min, Hl-7701 cells incubated with P (10 μM) for additional 30 min; (**e**) image of bright field cells in panel (**d**); (**f**) images of overlay in panels (**d**,**e**).

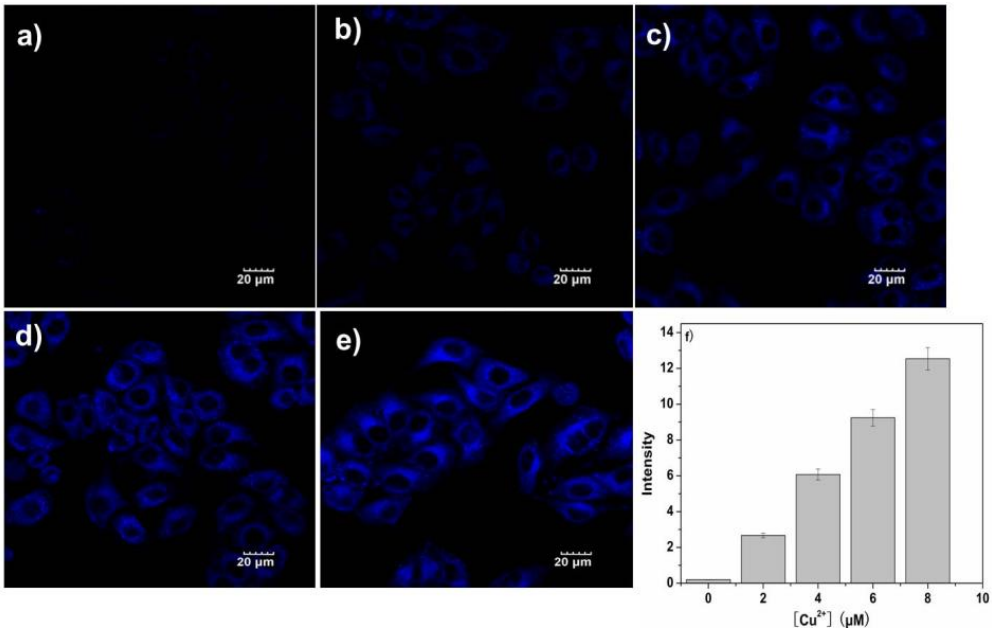

Figure 6. Confocal fluorescence images of Hela cells. (**a**–**e**): cells supplemented with 0, 2, 4, 6, 8 μM Cu^{2+} in the growth media for 30 min at 37 °C, and then incubated with 10 μM P for 30 min respectively; (**f**) fluorescence intensity of P with various [Cu^{2+}] ((**a**–**e**): 0, 2, 4, 6, 8 μM).

The subcellular localization of P in Hela cells was also conducted, Green 488 was selected as a nuclear dye. Afterwards, Hela cells were co-cultured with Cu^{2+} (10 μM), P (10 μM) and Green 488 in the growth medium as shown in Figure 5. The fluorescence imaging was recorded as represented in Figure 7, P (blue panel, Figure 7a) located in the periphery of Green 488 (green panel, Figure 7b); we concluded that P was mainly located in the cytoplasm of living cells as shown in Figure 7c.

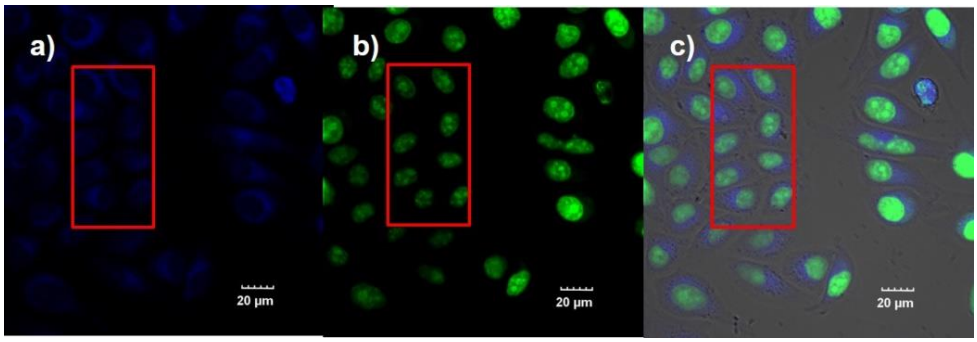

Figure 7. Subcellular localization of P in Hela cells. (**a**) cells supplemented with Cu^{2+} 10 μM) for 30 min, followed by the incubation with P 10 μM) for 30 min; (**b**) cells treated upon addition of Cu^{2+} (10 μM) for 30 min, P (10 μM) for another 30 min, and then cultured with Green 488 for 30 min; (**c**) images of overlay in panel (**a**,**b**).

Furthermore, the cytoplasm location of P in living Hela cells was also explored by conducting co-localization experiment (Figure 8). Mito Tracker Red and Green 488 were utilized as a mitochondria-specific dye and a nuclear-specific dye, respectively. The cell image of probe P (red panel, Figure 8a) and dye Mito Tracker Red (blue panel, Figure 8b) could not overlay completely in mitochondria (Figure 8d), so it could be concluded that probe P was not locate in mitochondria of Hela cells.

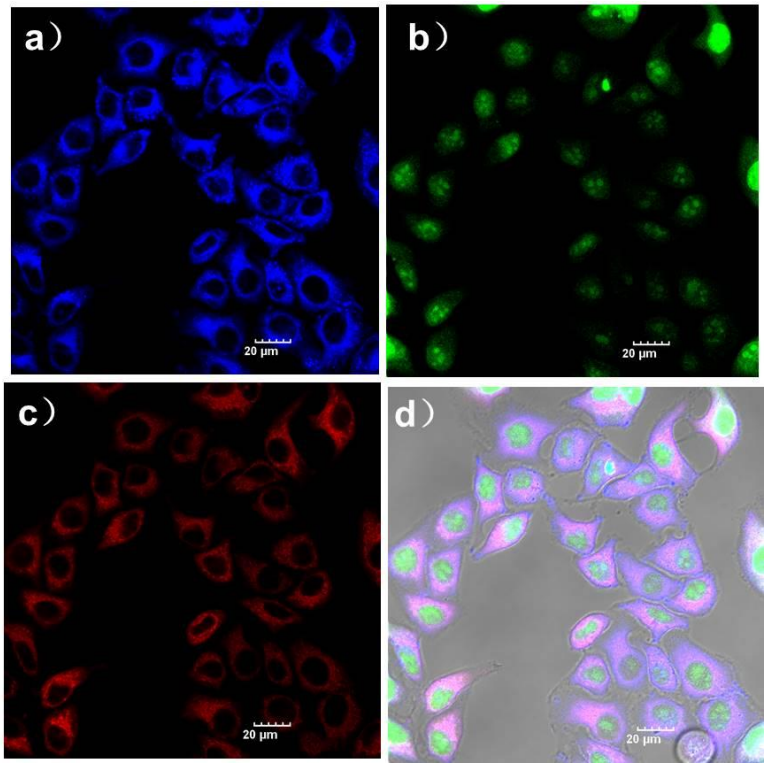

Figure 8. Cell localization experiment. (**a**) Cells were incubated with P for 30 min, and then Cu^{2+} (10 μM) for 30 min; (**b**) cells were incubated with P for 30 min, Cu^{2+} (10 μM) for 30 min, and Mito Tracker Red for 20 min at 37 °C, subsequently; (**c**) cells were incubated with P for 30 min, Cu^{2+} (10 μM) for 30 min, and Mito Tracker Red for 20 min at 37 °C, Green-488 for 10 min at 37 °C subsequently; (**d**) overlay field image of cells in panels (**a**–**c**).

3.6. Method Performance Comparison

The photophysical properties of reported probes and our proposed P toward Cu^{2+} were summarized as displayed in Table 1. Probes derived from different fluorophores, including spiropyran, pyridine, naphthalene, rhodamine and pyrene, exhibited fluorescence enhancement or quench which possessed good selectivity and high sensitivity, low LOD [24,32–35], and meanwhile most Cu^{2+}-probes can adopt dual signal changes towards Cu^{2+} except some probes [15,33,35,36]. Especially, some Cu^{2+} probes could display a ratiometric fluorescence change [32,35,37] as well as our proposed probe. Though the availability of fluorescence is increasing, there are still numerous challenges in developing new fluorescent probes for practical applications, such as unfavorable signal mode [15,34] rigorous testing media [15,36,37], no applicability [15,24,33–37] and narrow linear range [35]. Our newly designed pyrene-based probe possessed several advantages such as good selectivity and high sensitivity, a ratiometric dual fluorescence and wide linear range, encouraging applicability.

Table 1. Performances comparison of various fluorescent probes for Cu^{2+}.

Modes	Reagents	Selectivity	Linear Range (μM)	LOD (μM)	Testing Media	Applications	Remarks	Ref.
Quenching $\lambda_{ex}/_{em}$ = 556/603 nm	Spiropyran derivative	Good	0.75–3.6	0.15	Ethanol or pH 6.98 (0.1 M Tris-HCl)	NA	Fluorescence changes	[15]
Enhancement $\lambda_{ex}/_{em}$ = 530/580 nm	Rhodamingt derivative	Good	0.05–0.9	0.03	Water/methanol (1:4, *v*/*v*, pH 6.0, 20 mM HEPES)	NA	Dual chromo- and fluorogenic changes	[24]
Enhancement $\lambda_{ex}/_{em}$ = 342/375–460 nm	pyridine derivative	Good	0.1–20	0.02	Tris-HNO_3 (9:1 *v*/*v*, pH 7.0)	Water samples and living cells	Dual chromo- and fluorogenic changes, ratiometric.	[32]
Enhancement $\lambda_{ex}/_{em}$ = 370/410–415 nm	Pyrene derivative	Good	0.1–1.9	0.000234	Water/DMF solution (1:1, *v*/*v*)	NA	fluorogenic changes	[33]
Quenching $\lambda_{ex}/_{em}$ = 355/565 nm	Coumarin derivative	Good	0.5–4.5	0.0634	HEPES aqueous buffer (pH 7.0)	NA	Dual chromo- and fluorogenic changes	[34]
Enhancement $\lambda_{ex}/_{em}$ = 451/475–525 nm	Naphthalimide derivative	Good	0–0.1	0.01	Water-ethanol (6:4, *v*/*v*, pH 7.2, 50 mM HEPES)	NA	Fluorescent change, ratiometric	[35]
Enhancement $\lambda_{ex}/_{em}$ = 350/495 nm	Pyrene derivative	Good	NA	0.15	CH_3CN	NA	fluorogenic changes	[36]
Enhancement $\lambda_{ex}/_{em}$ = 360/430–489 nm	Naphthalimidet derivative	Good	NA	NA	CH_3CN	NA	Dual chromo- and fluorogenic changes, ratiometric	[37]
Enhancement $\lambda_{ex}/_{em}$ = 350/393–415 nm	Pyrene derivative	Good	0.5–8	0.16	Alcohol–water media (*v*/*v*, 8:2, pH 6.3, 20 mM HEPES)	Cell imaging	Dual chromo-and fluorogenic changes, ratiometric	This work

4. Conclusions

In summary, we took advantage of C=N isomerization and PET mechanism to design and synthesize facilely a newly pyrene-based probe for Cu^{2+}. The formation of P-Cu^{2+} complex effectively led to the enhanced fluorescence response of pyrene moiety, which realized ratiometric detection of Cu^{2+}. The probe exhibited an excellent feature of a dual-responsive colorimetric and fluorescent response to Cu^{2+}, which showed a high selectivity for Cu^{2+} compared with other metal ions in alcohol–aqueous media (*v*/*v*, 8:2, pH 6.3, 0.02 M HEPES). The proposed probe can be applied to the quantification of Cu^{2+} with a linear range

of 0.5–8 μM and the detection limit of 0.16 μM, and it was also applied for the imaging of Cu^{2+} in living cells, which showed P had low toxicity and good cytocompatibility. Further investigations on its applications in life science are still underway. We believe that the design concept should provide reference to develop new "off-on" probes for transition metal ions.

Supplementary Materials: The following supporting information can be downloaded at: https://www.mdpi.com/article/10.3390/chemosensors10060207/s1. Figure S1: MS spectra of P; Figure S2: ^{1}H NMR spectrum of P; Figure S3: ^{13}C NMR spectrum of P; Figure S4: MS spectra of P1; Figure S5: Fluorescence interfering experiment; Figure S6: Job's plot for P and Cu^{2+}; Figure S7: Benesi–Hildebrand plot between P and Cu^{2+}. Figure S8: MS spectra of P-Cu^{2+}; Figure S9: MTT experiment.

Author Contributions: Validation, data curation and writing—review and editing, C.Y.; Data curation, methodology and writing—original draft preparation, M.Y.; Validation, writing—original draft preparation and software, S.C.; Software, methodology and validation, Y.J.; Project management and funding acquisition, J.Z. All authors have read and agreed to the published version of the manuscript.

Funding: This work was financially supported by Hainan Province Science and Technology Special Fund (No. ZDYF2022SHFZ076) and the Natural Science Foundation of Hainan Province (No. 820RC626, No. 821RC559) and the National Natural Science Foundation of China (No. 81860381).

Institutional Review Board Statement: Not applicable.

Informed Consent Statement: Not applicable.

Data Availability Statement: Not applicable.

Conflicts of Interest: The authors declare no conflict of interest.

References

1. Que, E.L.; Domaille, D.W.; Chang, C.J. Metals in neurobiology: Probing their chemistry and biology with molecular imaging. *Chem. Rev.* **2018**, *108*, 1517–1549. [CrossRef] [PubMed]
2. Valeur, B.; Leray, I. Design principles of fluorescent molecular sensors for cation recognition. *Chem. Rev.* **2000**, *205*, 3–40. [CrossRef]
3. Barranguet, C.; Van den Ende, F.P.; Rutgers, M.; Breure, A.M.; Greijdanus, M.; Sinke, J.J.; Admiraal, W. Copper-induced modifications of the trophic relations in riverine algal-bacterial biofilms. *Environ. Toxicol. Chem.* **2003**, *22*, 1340–1349. [CrossRef] [PubMed]
4. Bhardwaj, V.; Nurchi, V.M.; Sahoo, S.K. Mercury toxicity and detection using chromo-fluorogenic chemosensors. *Pharmaceuticals* **2021**, *14*, 123. [CrossRef] [PubMed]
5. More, K.N.; Lim, T.H.; Kang, J.; Yun, H.; Yee, S.T.; Chang, D.J. Asymmetric and reduced xanthene fluorophores: Synthesis, photochemical properties, and application to activatable fluorescent probes for detection of nitroreductase. *Molecules* **2019**, *24*, 3206. [CrossRef]
6. Zheng, Q.; Ding, F.; Hu, X.; Feng, J.; He, X. ESIPT-based fluorescent probe for bioimaging and identification of group IIIA ions in live cells and zebrafish. *Bioorg. Chem.* **2021**, *109*, 104746. [CrossRef]
7. Huang, K.; Han, D.; Li, X.; Peng, M.; Zeng, X.; Jiang, L.; Qin, D. A new Cu^{2+}-selective fluorescent probe with six-membered spirocyclic hydrazide and its application in cell imaging. *Dyes Pigm.* **2019**, *171*, 107701. [CrossRef]
8. Liu, Y.; Su, Q.; Chen, M.; Dong, Y.; Shi, Y.; Feng, W.; Wu, Z.Y.; Li, F. Near-infrared upconversion chemodosimeter for in vivo detection of Cu^{2+} in Wilson disease. *Adv. Mater.* **2016**, *28*, 6625–6630. [CrossRef]
9. Chen, F.; Xiao, F.; Zhang, W.; Lin, C.; Wu, Y. Highly stable and NIR luminescent Ru-LPMSN hybrid materials for sensitive detection of Cu^{2+} in vivo. *ACS Appl. Mater. Int.* **2018**, *10*, 26964–26971. [CrossRef]
10. Wen, T.; Li, N.B.; Luo, H.Q. A turn-off fluorescent sensor for detecting Cu^{2+} based on fluorophore-labeled DNA and polyethyleneimine. *Sens. Actuators B-Chem.* **2014**, *192*, 673–679. [CrossRef]
11. Zhang, S.R.; Wang, Q.; Tian, G.H.; Ge, H.G. A fluorescent turn-off/on method or detection of Cu^{2+} and oxalate using carbon dots as fluorescent probes in aqueous solution. *Mater. Lett.* **2014**, *115*, 233–236. [CrossRef]
12. Huang, C.B.; Li, H.R.; Luo, Y.Y.; Xu, L. A naphthalimide-based bifunctional fluorescent probe for the differential detection of Hg^{2+} and Cu^{2+} in aqueous solution. *Dalton Trans.* **2014**, *43*, 8102–8108. [CrossRef] [PubMed]
13. Zhao, J.; Wang, Y.Y.; Chen, W.L.; Hao, G.S.; Sun, J.P.; Shi, Q.F.; Tian, F.; Ma, R.T. A salicylaldehyde benzoyl hydrazone based near-infrared probe for copper(II) and its bioimaging applications. *RSC Adv.* **2022**, *12*, 3073–3080. [CrossRef] [PubMed]
14. Li, Y.; Sun, M.; Zhang, K.; Zhang, Y.; Yan, Y.; Lei, K.; Wu, L.; Yu, H.; Wang, S. A near-infrared fluorescent probe for Cu^{2+} in living cells based on coordination effect. *Sens. Actuators B-Chem.* **2017**, *243*, 36–42. [CrossRef]
15. Shao, N.; Zhang, Y.; Cheung, S.M.; Yang, R.H.; Chan, W.H.; Mo, T.; Li, K.A.; Liu, F. Copper ion selective fluorescent sensor based on the inner filter effect using a spiropyran derivative. *Anal. Chem.* **2005**, *77*, 7294–7303. [CrossRef]

16. Kim, S.H.; Kim, J.S.; Park, S.M.; Chang, S.K. Hg^{2+}-selective off-on and Cu^{2+}-selective on-off type fluoroionophore based upon cyclam. *Org. Lett.* **2006**, *8*, 371–374. [CrossRef]
17. Luo, Y.; Li, Y.; Lv, B.Q.; Zhou, Z.D.; Xiao, D.; Choi, M.M.F. A new luminol derivative as a fluorescent probe for trace analysis of copper(II). *Microchim. Acta* **2009**, *164*, 411–417. [CrossRef]
18. Yu, C.W.; Wang, T.; Xu, K.; Zhao, J.; Li, M.H.; Weng, S.X.; Zhang, J. Characterization of a highly Cu^{2+}-selective fluorescent probe derived from rhodamine B. *Dyes Pigm.* **2013**, *96*, 38–44. [CrossRef]
19. Tang, L.J.; Zhou, P.; Zhong, K.L.; Hou, S.H. Fluorescence relay enhancement sequential recognition of Cu^{2+} and CN^{-} by a new quinazoline derivative. *Sens. Actuators B-Chem.* **2013**, *182*, 439–445. [CrossRef]
20. Yu, M.M.; Yuan, R.L.; Shi, C.X.; Zhou, W.; Wei, L.H.; Li, Z.X. 1,8-Naphthyridine and 8-hydroxyquinoline modified rhodamine B derivatives: "Turn-on" fluorescent and colorimetric sensors for Al^{3+} and Cu^{2+}. *Dyes Pigm.* **2013**, *99*, 887–894. [CrossRef]
21. You, Q.H.; Zhuo, Y.H.; Feng, Y.D.; Xiao, Y.J.; Zhang, Y.Y.; Zhang, L. A highly selective fluorescent probe for the sensing of Cu^{2+} based on the hydrolysis of a quinoline-2-carboxylate and its application in cell imaging. *J. Chem. Res.* **2021**, *45*, 315–321. [CrossRef]
22. Yu, C.W.; Chen, L.X.; Zhang, J.; Li, J.H.; Liu, P.; Wang, W.H.; Yan, B. "Off-on" based fluorescent chemosensor for Cu^{2+} in aqueous media and living cells. *Talanta* **2011**, *85*, 1627–1633. [CrossRef] [PubMed]
23. Zhao, Y.H.; Luo, Y.Y.; Wang, H.; Wei, H.P.; Guo, T.; Tan, H.L.; Yuan, L.; Zhang, X.B. A novel ratiometric and reversible fluorescence probe with a large Stokes shift for Cu^{2+} based on a new clamp-on unit. *Anal. Chim. Acta* **2019**, *1065*, 134–141. [CrossRef] [PubMed]
24. Yu, C.W.; Zhang, J.; Wang, R.; Chen, L.X. Highly sensitive and selective colorimetric and off-on fluorescent probe for Cu^{2+} based on rhodamine derivative. *Org. Biomol. Chem.* **2010**, *8*, 5277–5279. [CrossRef]
25. Long, S.S.; Qiao, Q.L.; Miao, L.; Xu, Z.C. A self-assembly/disassembly two-photo ratiometric fluorogenic probe for bacteria imaging. *Chin. Chem. Lett.* **2019**, *30*, 573–576. [CrossRef]
26. Chao, J.; Wang, Z.; Zhang, Y.; Huo, F.; Duan, Y. A pyrene-based fluorescent probe for specific detection of cysteine and its application in living cell. *J. Fluoresc.* **2021**, *31*, 727–732. [CrossRef]
27. Xu, Y.; Yang, L.; Wang, H.; Zhang, Y.; Yang, X.; Pei, M.; Zhang, G. A new "off-on-off" sensor for sequential detection of Al^{3+} and Cu^{2+} with excellent sensitivity and selectivity based on different sensing mechanisms. *J. Photochem. Photobiol. A* **2020**, *391*, 112372. [CrossRef]
28. Wu, J.S.; Liu, W.M.; Zhuang, X.Q.; Wang, F.; Wang, P.F.; Tao, S.L.; Zhang, X.H.; Wu, S.K.; Lee, S.T. Fluorescence turn on of coumarin derivatives by metal cations: A new signaling mechanism based on C=N isomerization. *Org. Lett.* **2007**, *9*, 33–36. [CrossRef]
29. Sheng, J.R.; Feng, F.; Qiang, Y.; Liang, F.G.; Sen, L.; Wei, F.H. A coumarin-derived fluorescence chemosensors selective for copper(II). *Anal. Lett.* **2008**, *41*, 2203–2213. [CrossRef]
30. WHO. *Guidelines for Drinking-Water Quality*, 3rd ed.; WHO: Geneva, Switzerland, 2008.
31. Rodríguez-Cáceres, M.I.; Agbaria, R.A.; Warner, I.M. Fluorescence of metal-ligand complexes of mono- and di-substituted naphthalene derivatives. *J. Fluoresc.* **2005**, *15*, 185–190. [CrossRef]
32. Wu, Y.S.; Li, C.Y.; Li, Y.F.; Li, D.; Li, Z. Development of a simple pyrene-based ratiometric fluorescent chemosensor for copper ion in living cells. *Sens. Actuators B-Chem.* **2016**, *222*, 1226–1232. [CrossRef]
33. Choi, N.G.; Vanjare, B.D.; Mahajan, P.G.; Nagarajan, R.; Ryoo, H.I.; Lee, K.H. Schiff base functionalized 1,2,4-Triazole and pyrene derivative for selective and sensitive detection of Cu^{2+} ion in the mixed organic-aqueous media. *J. Fluoresc.* **2021**, *31*, 1739–1749. [CrossRef] [PubMed]
34. Chao, J.B.; Zhang, Y.; Wang, H.F.; Zhang, Y.B.; Huo, F.J.; Yin, C.X.; Qin, L.P.; Wang, Y. A coumarin-based fluorescent probe for selective detection of Cu^{2+} in water. *J. Coord. Chem.* **2013**, *66*, 3857–3867. [CrossRef]
35. Xu, Z.C.; Xiao, Y.; Qian, X.H.; Cui, J.N.; Cui, D.W. Ratiometric and selective fluorescent sensor for CuII based on internal charge transfer (ICT). *Org. Lett.* **2005**, *7*, 889–892. [CrossRef] [PubMed]
36. Hazarika, S.I.; Mahata, G.; Pahari, P.; Pramanik, N.; Atta, A.K. A simple triazole-linked bispyrenyl-based xylofuranose derivative for selective and sensitive fluorometric detection of Cu^{2+}. *Inorg. Chim. Acta* **2020**, *507*, 119582. [CrossRef]
37. Xu, Z.; Han, S.J.; Lee, C.; Yoon, J.; Spring, D.R. Development of off–on fluorescent probes for heavy and transition metal ions. *Chem. Commun.* **2010**, *46*, 1679–1681. [CrossRef]